

Energy Based Path Planning for a Novel Cabled Robotic System

Per Henrik Borgstrom*, Amarjeet Singh*, Brett L. Jordan[†], Gaurav S. Sukhatme[‡],
Maxim A. Batalin[§] and William J. Kaiser*

*Department of Electrical Engineering, University of California, Los Angeles

[†]Department of Mechanical Engineering, University of California, Los Angeles

[‡]Department of Computer Science, University of Southern California

[§]Center for Embedded Networked Sensing, University of California, Los Angeles

Email: hborgstr@ucla.edu

Abstract—Cabled robotic systems have been used for a diverse set of applications such as environmental sensing, search and rescue, sports and entertainment and air vehicle simulators. In this paper, we introduce a new cabled robot- Networked Info Mechanical System for Planar actuation (NIMS-PL), with energy profiling capabilities. Accurate energy measurements supported by NIMS-PL enable path planning that optimizes the robot's path subject to an upper bound on energy consumption. We performed extensive empirical validation of the optimized path planning approach in simulation using an environmental sensing application as an example. We also validated the simulation results using NIMS-PL, demonstrating significant improvements in the sensing task when accounting with accurate energy measurements as opposed to Euclidean distance, which is typically used for modeling energy spent in path traversal.

I. INTRODUCTION

Mobile robotic systems have been used for a diverse set of applications including mapping, search and exploration, environmental sensing, security, home automation, industrial automation and healthcare. Large spatial coverage and dynamic temporal variations associated with many such applications along with the limited energy capacity of the mobile robots makes it critical to perform careful path planning. Optimizing the collected information while accounting for the *path cost* is a well studied problem in Operations Research (as Traveling Salesman Problem with Profits and its variant) [1], in theoretical computer science [2] and in robotics [3], [4], [5], [6].

In this paper, we focus on environmental sensing applications while performing path planning with a new proposed cabled robotic system. Environmental sensing applications involve one or multiple robots equipped with sensors that measure an environmental variable of interest. The goal might be to reconstruct the phenomenon associated with this variable or to capture events exhibited by it. However, it should be noted that the proposed approach can be directly used for other robotic applications that require path planning under energy constraints, especially when the energy metric is not a linear function.

For efficient path planning in environmental sensing applications, Singh et. al [3] modeled phenomena as a Gaussian Process (GP) and provided a theoretical framework. While the approach in [3] is independent of the cost model used for modeling the traveling cost between

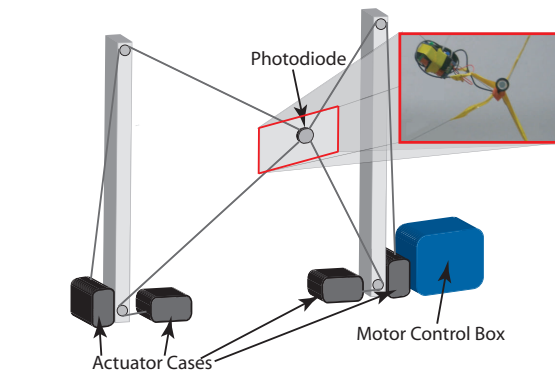


Fig. 1: Schematic of a NIMS-PL system actuating an optical sensor in a vertical plane while observing light intensity

a given set of locations, it uses Euclidean distance as a measure of traveling cost. Zhang et. al [4] studied the problem of estimating a scalar field using local linear regression. Their approach uses distance traversed in a circular arc based on minimum turning radius and speed while optimizing the expended energy as path cost.

Many robotic sampling tasks are performed in environments with limited energy availability. In such cases, energy constraints may limit deployment lifetime, and it is critical that the robot traverse energy efficient paths in order to maximize sensing utility. Mei et. al [5] considered the effect of scaling velocity and changes in direction and acceleration in energy accounting for paths traversed by a mobile robot. They extended their work in [6] to incorporate energy accounting during exploration while deciding the next target location to explore based on partial information already acquired about the environment.

While there has been significant research performed in energy efficient path planning for mobile robotic systems, little work has been done in energy accounting for path planning in cabled robotic systems. Cabled robotic systems have been used for a diverse set of applications such as environmental sensing [7], search and rescue [8], sports and entertainment [9], [10] and air vehicle simulators [11]. Stealey et. al [7] performed path planning based on the approach discussed in [3] using Aquatic Networked InfoMechanical System (NIMS-AQ), a tethered robotic system designed specifically for sensing applications in aquatic environments.

Borgstrom et. al [12] proposed NIMS-3D, a new system in

the NIMS family of tethered systems capable of actuation in a three dimensional environment. In [13], the work proposed in [12] is extended, and an algorithm for generating energy efficient trajectories for NIMS-3D is proposed. The algorithm generates energy-efficient non-linear trajectories for motion between given locations in an unobstructed workspace.

In this paper we propose Networked InfoMechanical System for Planar actuation (NIMS-PL), a four-cabled robotic platform used for actuation in planar workspaces. It is intended for actuated sensing applications in both terrestrial and aquatic environments. Real time energy profiling enables energy-based path planning - maximizing the collected information while constraining the total energy expenditure. To this end, we use the approach discussed in [3] to model the phenomena as a Gaussian Process and use mutual information between the visited locations and the remainder of the space to quantify the amount of information collected. We precompute the energy costs associated with each path using a model for the actuator systems and use these energy values as a model for path cost. Thereafter, a path planning algorithm known as *Orienteering algorithm* (OP), as proposed in [14], is used to maximize the collected information subject to upper bounds on energy consumption.

We present extensive empirical analysis comparing energy and Euclidean distance as the cost models for path planning using the OP algorithm. We demonstrate that paths evaluated using distance as the model for path cost can be inefficient in terms of total energy consumption. Furthermore, we also provide extensive validation of our approach on NIMS-PL. More specifically, the contributions of this paper are:

- Development of NIMS-PL, a four-cabled robotic system with accurate, real time energy profiling capabilities used for actuation in planar workspaces
- Performing *path planning* using actual energy measurements as the model for *path cost*
- Demonstration of energy inefficiency in using Euclidean distance as a cost model while performing path planning for cabled robots
- Extensive validation of our approach on NIMS-PL

II. ROBOTIC PLATFORM

We have developed NIMS-PL, a cabled robotic system with energy profiling capabilities used for actuation in planar workspaces. Four tension controlled cables actuate a generic sensor to provide planar spatial coverage. Planar operation is feasible both in a vertical plane, as well as in a horizontal plane for aquatic applications with a buoyant sensor node supported by the water surface. The four cabled configuration enables quadrangular workspaces, thus allowing a larger feasible workspace as compared to a three cabled configuration. Additionally, large spatial coverage is possible in aquatic deployments, since the weight of the end-effector does not need to be supported by the cables. A schematic of NIMS-PL system actuating an optical sensor in a vertical plane while observing light intensity is shown in Fig. 1.

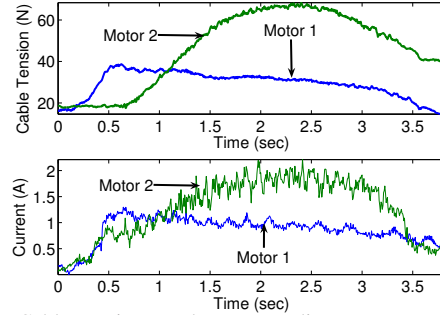


Fig. 2: Cable tensions and corresponding motor currents during example move

A. Model of Actuator Systems

In order to estimate the energy cost associated with a trajectory, it is necessary to develop a model of its actuator systems. The actuators in our robot are brushless DC servomotors that are driven by means of PWM controlled H-bridges [15]. These motors are governed by the relations given in Eq. (1) and (2) [16].

$$V(t) = L \frac{\partial I(t)}{\partial t} + RI(t) + K_E \omega \quad (1)$$

$$\tau(t) = K_T I(t) \quad (2)$$

where $V(t)$ is the applied voltage, $I(t)$ is actuator current, L and R are the armature inductance and resistance respectively, τ is torque, ω is motor speed, and K_T and K_E are motor constants that are equal in SI units. For the sake of simplicity, we make a quasi static approximation, thereby taking time derivatives as zero. Therefore, after dropping the $L \frac{\partial I(t)}{\partial t}$ term, manipulation of Eqn. (1) and (2) yields:

$$VI = \tau\omega + I^2R = \tau\omega + IR \frac{\tau}{K_T} \quad (3)$$

where VI is electrical power, $\tau\omega$ is power delivered to the load, and I^2R is ohmic loss in the armature resistance. I^2R loss is the primary source of inefficiency in the actuators and is therefore the energy cost that we seek to minimize.

We have from Eqn. (2) that armature current scales directly with motor torque. In a cabled robotic system with ideal actuators, the motor torque scales directly with the tension in the cable that is regulated by the motor. However, our actuators have built-in gearboxes, which cause friction and result in some deviation from the relationship in Eqn. (2). A plot of cable tensions and armature current for the two actuators during an example move is illustrated in Fig. 2. The relationship between cable tension and armature current appears roughly linear, although some nonlinearity is evident in the trace of motor 2 current. In this work, however, we adopt the approximation of Eqn. (2), thereby assuming that I^2R loss scales in direct proportion with the square of cable tension. Experimental results, given in Section IV, indicate that this approximation does not adversely affect energy budgeting capabilities.

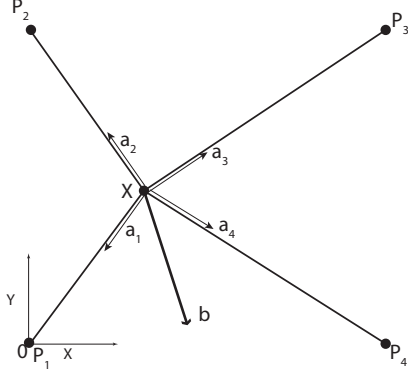


Fig. 3: Kinematic diagram of a NIMS-PL configuration showing \vec{a}_i , P_i , X , and an example desired force vector, \vec{b}

B. Optimal Tension Distribution

The sensor node can be actuated by regulating the tensions in the set of supporting cables. As an illustration, consider the configuration shown in Fig. 3, with cable origins given by $P_{1\dots 4}$, node position given by $X = [x \ y]^T$, and a desired force vector \vec{b} , that is to be imparted on the end-effector. The set of tension distributions that provide the appropriate net force on the end-effector is characterized by:

$$AT = \vec{b} \quad (4)$$

where $T = [T_1 \ T_2 \ T_3 \ T_4]^T$ is the set of cable tensions and A is a pose-dependent structure matrix. The i^{th} column of A is given by $\vec{a}_i = \frac{P_i - X}{\|P_i - X\|}$, the unit vector from the X to P_i , i.e.:

$$A = [\vec{a}_1 \ \vec{a}_2 \ \vec{a}_3 \ \vec{a}_4] \quad (5)$$

Since A is a 2×4 matrix, Eqn. (4) is underdetermined. Thus, it is apparent that using four cables to control two degrees of freedom results in two degrees of dynamic redundancy. This results in an infinite number of tension distributions that satisfy the equality condition.

The most significant difference between cabled robots and solid arm parallel mechanisms is the inability of cables to exert positive or push forces. Thus, in finding a valid tension distribution in Eqn. (4), it becomes necessary to bound the set of tensions between T_{min} and T_{max} , the lower and upper bound on the tension. The lower bound is required to protect against cable slack, and the upper bound is a result of the finite torque capabilities of the system's actuators. Finding the one-norm optimal set of valid tension distributions can then be expressed as follows:

$$T^* = \text{argmin } \mathbf{1}^T T$$

s.t.

$$\begin{aligned} (1) \quad & AT = \vec{b} \\ (2) \quad & T_{min} \leq T \leq T_{max} \end{aligned} \quad (6)$$

This is immediately recognizable as a Linear Programming formulation, which we solve by means of a novel algorithm similar to the standard *simplex* method [17].

The optimal set of tensions, T^* , is a function of position and the desired force vector \vec{b} . Fig. 4 shows the two-norm

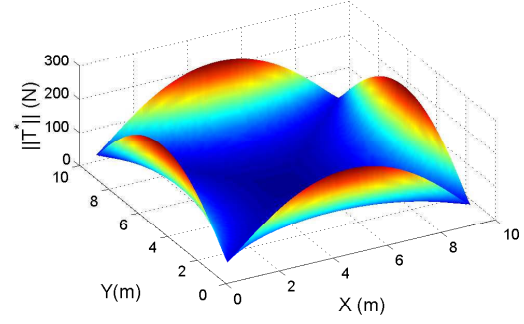


Fig. 4: $\|T^*\|_2$ shown against location in the workspace for static NIMS-PL configurations

of the tension vector, $\|T^*\|_2$, as a function of position in a hypothetical $10m \times 10m$ configuration with the desired force vector $\vec{b} = 0$. It is evident that the central region and corners of the workspace are characterized by low tensions, while the edges are characterized by significantly higher tensions.

C. Estimating Trajectory Energy Cost

The energy loss associated with executing a trajectory can be found by integrating the I^2R loss over the duration of the trajectory, i.e.:

$$E = \int_{t=0}^{t=t_f} R \|\vec{I}(X(t), \vec{b}(t))\|^2 dt \quad (7)$$

where $\vec{I} = [I_1 \ I_2 \ I_3 \ I_4]^T$ is the set of motor currents. Eqn. (2) indicates that armature current is directly related to motor torque. Since motor torque is directly related to cable tension, Eqn. (7) can be rewritten as:

$$\begin{aligned} E &= \int_{t=0}^{t=t_f} R \|KT^*(X(t), \vec{b}(t))\|^2 dt \\ &= K^2 R \int_{t=0}^{t=t_f} \|T^*(t)\|^2 dt \end{aligned} \quad (8)$$

where K is a coefficient relating armature current and cable tension by the linear relation $I = KT$.

$T^*(t)$ is a function of position, $X(t)$, and the force vector, $\vec{b}(t)$, required to accelerate the sensor node and counteract any frictional forces acting on it. For example, the most significant frictional force in aquatic environments is generated by hydrodynamic friction. Hydrodynamic friction can be modeled as a sum of first and higher order functions of velocity [18]. Since the operating speed of NIMS-PL is generally low, ignoring the effects of water friction will not introduce significant error into the analysis. Thus, $\vec{b} \approx m\vec{a}$, where \vec{a} is the acceleration vector of the end-effector.

From Eqn. (8), we have that the energy cost associated with a trajectory scales with the square of the two-norm of the vector of cable tensions. The results shown in Fig. 4 can now be interpreted as follows: Operating near the center or in the corners of the workspace results in low cable tensions and thereby low power consumption, whereas operating near its edges yields high cable tensions and thus large I^2R power loss. Therefore, an intelligent sampling strategy



Fig. 5: Light intensity pattern used as representative of sensing phenomena

should exploit the low operating power associated with the middle of the workspace and avoid the poor energy efficiency associated with the edges of the workspace.

D. System Hardware

NIMS-PL is implemented using 520W DC servomotors with built-in 3:1 gear heads[19]. Their peak torque is $3.27Nm$, and the rated speed is 5800 rpm. Thus they are sufficiently powerful for large scale deployments required for many environmental sampling applications we envision. These actuators are controlled by a Delta Tau stand-alone four axis controller with integrated PWM amplifiers [15]. This device features built-in current sensors, which we use in determining trajectory energy cost. Tension control is also managed by this device, with feedback coming from cantilevered strain gauge transducers [20].

III. PATH PLANNING

Let us now formalize the *path planning* problem for the application scenario of actuating a NIMS-PL end-effector carrying a sensor in a two dimensional space. We assume that the spatial domain observed using NIMS-PL is discretized into finitely many sensing locations \mathcal{V} . For each subset $\mathcal{A} \subseteq \mathcal{V}$, let $I(\mathcal{A})$ denote the *sensing quality*, i.e. the informativeness, of observing the phenomenon at locations \mathcal{A} . Selection of the sensing quality is discussed in Section III-A. When traveling between two locations, u and v , NIMS-PL incurs a *traveling cost* $C(u, v) > 0$. NIMS-PL will traverse a *path* in this space: an s - t -path \mathcal{P} is a sequence of n locations starting at node s , and finishing at t . The cost $C(\mathcal{P})$ of the path $\mathcal{P} = (s = v_1, v_2, \dots, v_n = t)$ is the sum of traveling costs along the path, i.e., $C(\mathcal{P}) = \sum_{i=2}^n C(v_{i-1}, v_i)$. We use the notation \mathcal{P} to refer both to the sequence of nodes in the path, and to the subset of sensing locations $\mathcal{P} \subseteq \mathcal{V}$ (ignoring their sequence). $I(\mathcal{P})$ denotes the sensing quality of the traversed path \mathcal{P} .

The goal for the *path planning* problem is to find a path \mathcal{P} with specified starting and finishing locations s and t (not necessarily different), such that the path has bounded cost $C(\mathcal{P}) \leq B$ for some specified budget B , and that the path is the *most informative*, i.e., $I(\mathcal{P})$ is maximized. Formally, the problem can be defined as:

$$\max_{\mathcal{P} \subseteq \mathcal{V}} I(\mathcal{P}); \quad \text{subject to } C(\mathcal{P}) \leq B \quad (9)$$

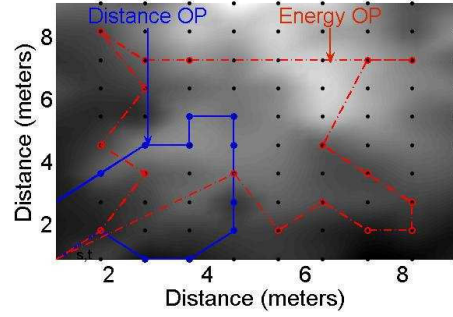


Fig. 6: Comparison of paths found using DOP and EOP for the initial budget constraint of 16 meters for Euclidean distance cost model

A. Quantifying informativeness

In modeling spatial phenomena, a common approach in statistics is to use a rich class of probabilistic models called *Gaussian Processes* (GPs, *c.f.*, [21]). Such models associate a random variable \mathcal{X}_v with each location $v \in \mathcal{V}$. The joint distribution $P(\mathcal{X}_{\mathcal{V}})$ can then be used to quantify uncertainty in the prediction $P(\mathcal{X}_{\mathcal{V} \setminus \mathcal{A}} | \mathcal{X}_{\mathcal{A}} = \mathbf{x}_{\mathcal{A}})$ of phenomena at unobserved locations $\mathcal{X}_{\mathcal{V} \setminus \mathcal{A}}$, after making observations $\mathcal{X}_{\mathcal{A}} = \mathbf{x}_{\mathcal{A}}$ at a small subset \mathcal{A} of locations. To quantify this uncertainty, we use the *mutual information* (MI) criterion defined in [22]. For a set of locations \mathcal{P} , the MI criterion is defined as:

$$I(\mathcal{A}) \equiv \text{MI}(\mathcal{A}) \equiv H(\mathcal{X}_{\mathcal{V} \setminus \mathcal{A}}) - H(\mathcal{X}_{\mathcal{V} \setminus \mathcal{A}} | \mathcal{X}_{\mathcal{A}}), \quad (10)$$

where $H(\mathcal{X}_{\mathcal{V} \setminus \mathcal{A}})$ is the entropy of the unobserved locations $\mathcal{V} \setminus \mathcal{A}$, and $H(\mathcal{X}_{\mathcal{V} \setminus \mathcal{A}} | \mathcal{X}_{\mathcal{A}})$ is the conditional entropy of locations $\mathcal{V} \setminus \mathcal{A}$ after sensing at locations \mathcal{A} . Hence, MI measures the reduction in uncertainty at the unobserved locations. Thus, we use MI as our measure of sensing quality in Eqn. (9). Conveniently, in a GP, the mutual information criterion can be computed efficiently and analytically [22]. A study of the effectiveness of mutual information in selecting informative sensing locations is presented in [23].

B. Orienteering Heuristic

Even if we do not consider the constraints on the length of the paths of the robots, the problem of selecting locations that maximize mutual information is NP-hard [23]. Hence, in general we cannot expect to efficiently find optimal paths. Instead, we use the *orienteering heuristic* (hereafter referred to as OP algorithm) discussed in [14] to efficiently compute suboptimal paths. This method has been empirically found to be one of the best heuristics for a similar problem setting [24] and has furthermore been used in the approximation algorithm proposed in [3] for the same path planning problem. For the sake of completeness, we discuss here briefly the approach used in the heuristic for estimating efficient paths.

The OP algorithm consists of two steps: initialization and improvement. The solution is initialized by constructing an ellipse over the entire set of points by using the starting and finishing node as the two foci of the ellipse and the

available budget constraint as the length of the major axis. Only locations lying inside the ellipse satisfy the budget constraint requirement. Several paths are generated over this set of locations, whereafter the paths are subjected to exchange of locations between the paths, insertion/ deletion of locations within the path and finally moving the locations within the path resulting in improved collected reward and reduced path cost. In the improvement step, the total reward is allowed to decrease in the hope of ultimately finding a path with a larger total reward. Details of the OP algorithm are presented in [14]. It is important to note that, while this heuristic solves the path planning problem efficiently, it does not provide any performance guarantee. This further implies that an output path with a higher input budget constraint may collect lower total reward as compared to an output path with lower input budget constraint.

C. Path Planning using NIMS-PL

In this paper we evaluate two metrics and use them with the OP algorithm. The first version of the OP algorithm relies on Euclidean distance as the cost model and is unaware of energy consumption. Its goal is to maximize reward subject to a constraint on path length. We call this approach *Distance-OP* (DOP). We then compute the total energy consumption of each evaluated path. This value is then used as an upper bound while running the OP algorithm again with energy as model for path cost. We call this approach *Energy-OP* (EOP). With extensive empirical validation discussed in Section IV, we demonstrate that EOP provides significant improvement in energy efficiency over DOP.

IV. EXPERIMENTAL RESULTS

We performed extensive empirical evaluation of path planning using both the DOP and EOP methods. For the purpose of simulations, we computed the energy values for a hypothetical $10m \times 10m$ deployment characterized by maximum velocity $.5m/s$, maximum acceleration $.5m/s^2$, minimum cable tension $20N$, and maximum cable tension $200N$. Since the distribution of light intensity under a forest canopy provides a good example of an environmental phenomenon exhibiting spatial dynamics and is of interest to application scientists, we used an image captured under the forest canopy as a representative data set for our experiments.

Fig. 5 displays an image captured in James Forest Reserve (California) using a downlooking camera mounted on a tree. The image is converted into grayscale and divided into a 10×10 uniform grid. The average pixel intensity within each region on the grid is computed and taken as the observed intensity at the discrete locations on the grid. The background in Fig. 6 shows the interpolated grayscale image with the discrete observation locations as points.

To calculate information quality at each observation location, we learn a non stationary GP model using a covariance function parameterization as described in [25]. The parameters are chosen by maximizing the marginal likelihood [21]. This non-stationary process is learned by dividing the complete region into smaller sub-regions and

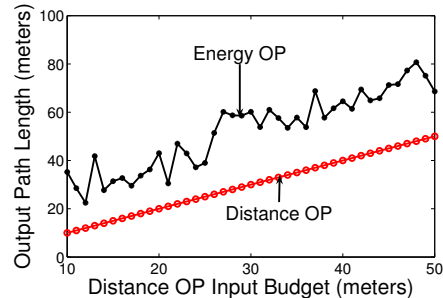


Fig. 7: Comparison of distances traveled by the DOP and EOP methods while expending equal total energy

combining the locally-stationary GPs from each of these sub regions. Using the learned GP model, we then find the information quality for each observation location by calculating the mutual information as discussed in Section III.

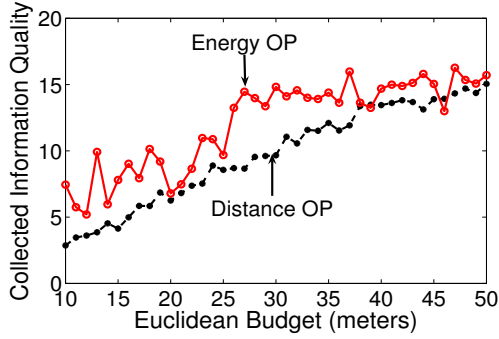
A. Simulation using real sensing data

In order to evaluate the DOP algorithm, we performed a series of simulations. We specified the bottom left position on the grid as both the starting and the finishing location and computed paths using the DOP algorithm while varying the upper bound on Euclidean path length from $10m$ to $50m$.

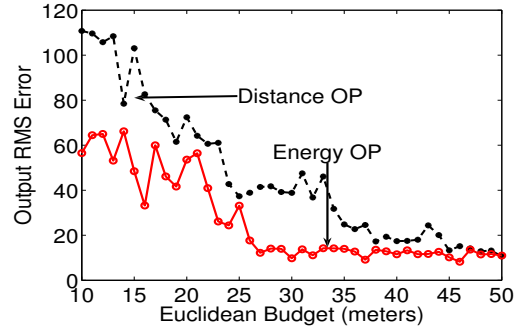
Upon computing these Euclidean distance based paths, we employed the EOP algorithm using the total energy cost of the DOP paths as upper bounds. Since the EOP strategy is aware of path energy costs, it favors locations in low power middle and corner regions of the workspace over high power edge regions. Consequently, these paths traverse much larger distances and collect more information for the same energy cost as compared to paths selected by DOP. A comparison of the total distance traversed for both cost models is shown in Fig. 7, and collected information gain is shown in Fig. 8a. A comparison of the paths found using both cost models for the initial distance constraint of $16m$ is shown in Fig. 6.

Using the observed values from the visited locations and the learned GP model, we predict light intensity at the unobserved locations. Thereafter, we calculate the root mean square (RMS) error between the predicted values and the actual intensity values at the unobserved locations. Fig. 8b compares the RMS values for DOP and EOP methods as the input budget constraint is varied. It is clear that the energy-aware metric outperforms the Euclidean distance metric. Furthermore, the two methods converge asymptotically at the far end of the budget spectrum as the search space is saturated.

The primary advantage of EOP as compared to DOP is that the energy cost of information is reduced. In other words, EOP reduces the energy cost of achieving a desired RMS error or a desired amount of mutual information. Fig. 9 shows RMS errors and energy costs associated with the simulated DOP and EOP paths. It is apparent the RMS error achieved by EOP paths is generally significantly lower than that achieved by DOP paths with the same energy cost. For this experiment, the EOP method reduces RMS error by an average of 48%.



(a) Comparison of collected information quality



(b) Comparison of Root Mean Square (RMS) error

Fig. 8: Comparison of simulation results for DOP and EOP methods

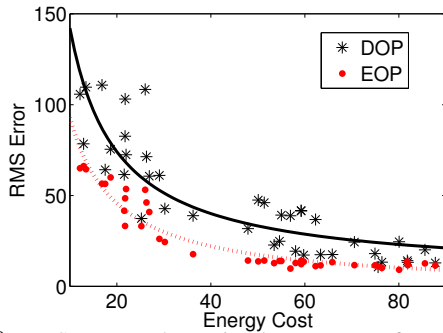


Fig. 9: RMS errors and associated energy costs for DOP and EOP methods

B. Experimental Results on NIMS-PL

We implemented the same set of experiments as performed in simulations on a lab scale NIMS-PL system with a vertical workspace of $1.264m \times 1.264m$. The grayscale image shown in the background of Fig. 6 was projected in the vertical workspace of the robot, and the end-effector was equipped with a photodiode for measuring the incident light intensity. Measurements were relayed to the backend by a Bluetooth transmitter. We first performed a complete scan of all the points on uniformly spaced 10×10 grid of observation locations in the workspace. The collected intensity data is used as the ground truth for learning the GP model and for RMS error calculations.

We then recomputed the paths using the DOP algorithm with the new GP model, using mutual information as the reward associated with each observation location. The expected total energy cost of these paths was computed and EOP was used to generate paths with these costs as energy budget. The paths calculated by the DOP and EOP methods were then executed on NIMS-PL, and light intensity was measured at each observation location along the paths. It should be noted that the input budget for the DOP paths was scaled by a factor of .1264 to account for the smaller size of the workspace.

Fig. 10a displays the comparison of collected information quality for DOP and EOP strategies while performing experiments with NIMS-PL. For large distance budgets, the paths selected by both methods span a large number of observation locations, thereby saturating the total collected information.

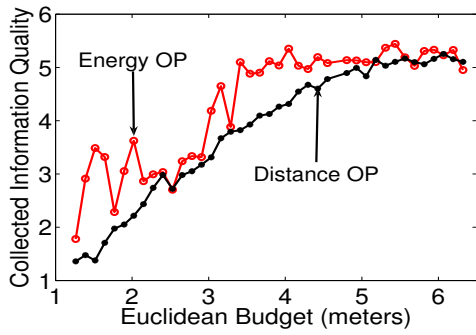
For smaller input budgets, it is apparent that the energy cost method always outperforms the Euclidean method.

The observed intensity values and the learned GP model were used to predict light intensity at unobserved locations. Fig. 10b compares the RMS error between the predicted intensity values and actual intensity values observed during the uniform scan. The asymptotic behavior in Fig. 10a is once again evident, as the RMS error becomes small for both methods as more locations are observed. For smaller input budgets, the EOP method typically demonstrates lower RMS error as compared to the DOP method. It should be noted here that the DOP method slightly outperforms the EOP method for input budgets between 2.1 and 3 meters. This is most likely caused by ambient noise: The collected light intensity data, which is used for learning the GP model, has inherent noise due to ambient light. When path planning is performed, a path is selected that maximizes the collected information as per the learned model. However, due to ambient noise, the path with higher information gain for the input budgets did not result in lower RMS error for this input budget range.

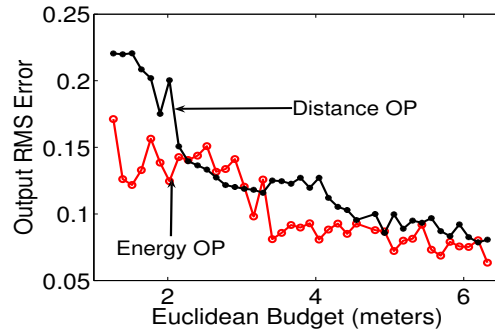
Fig. 11 compares the total I^2R energy cost associated with the paths for EOP and DOP methods as measured during execution of the paths. We expect the EOP method to consume almost all of its energy budget, and therefore expect the two plots to match each other closely. The values are in excellent agreement, indicating that adopting the ideal actuator approximation of Eqn. (2) does not adversely affect energy budgeting capabilities.

V. CONCLUSIONS AND FUTURE WORK

In this paper, we presented Networked InfoMechanical System for Planar actuation (NIMS-PL), a four cabled robotic platform with energy profiling capabilities used for actuation in planar workspaces. To demonstrate the utility of energy profiling, we performed energy based path planning - optimizing the path traversed by the robotic system subject to bounds on total energy consumption. To quantify the information quality associated with each observation location, we modeled the observed phenomena as a Gaussian Process and used mutual information as the criterion for information quality. We performed extensive empirical analysis, both in



(a) Comparison of collected information quality



(b) Comparison of Root Mean Square (RMS) error

Fig. 10: Comparison of DOP and EOP methods as executed on NIMS-PL

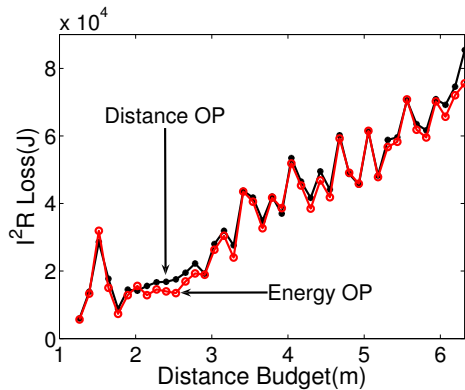


Fig. 11: Experimental I^2R loss for DOP and EOP methods

simulation and using NIMS-PL, to demonstrate that path planning using energy accounting outperforms methods using Euclidean distance as path cost.

In the future, we plan to compare the performance of other path planning approaches for NIMS-PL. We also plan to use NIMS-PL for monitoring in aquatic environments to provide accurate high resolution coverage over the water surface.

VI. ACKNOWLEDGMENTS

This material is based upon work supported in part by the US National Science Foundation (NSF) under Grants ANI-00331481 and ANI-331481. Any opinions, findings, and conclusions or recommendations expressed in this material are those of the authors and do not necessarily reflect the views of the NSF.

REFERENCES

- [1] D. Feillet, P. Dejax, and M. Gendreau, "Traveling salesman problem with profits," *Trans Sci*, vol. 39(2), pp. 188–205, '05.
- [2] A. Blum, S. Chawla, D. R. Karger, T. Lane, A. Meyerson, and M. Minkoff, "Approximation algorithms for orienteering and discounted-reward tsp," in *Foundations of Computer Science (FOCS)*, 2003, p. 46.
- [3] A. Singh, A. Krause, C. Guestrin, W. J. Kaiser, and M. A. Batalin, "Efficient planning of informative paths for multiple robots," in *International Joint Conference on Artificial Intelligence (IJCAI)*, Hyderabad, India, January 2007, pp. 2204–2211.
- [4] B. Zhang and G. S. Sukhatme, "Adaptive sampling for estimating a scalar field using a robotic boat and a sensor network," in *IEEE International Conference on Robotics and Automation*, 2007, pp. 3673–3680.

- [5] Y. Mei, Y.-H. Lu, Y. C. Hu, and C. G. Lee, "Energy-efficient motion planning for mobile robots," in *IEEE International Conference on Robotics and Automation*, 2004, pp. 4344–4349.
- [6] Y. Mei, Y.-H. Lu, C. G. Lee, and Y. C. Hu, "Energy-efficient mobile robot exploration," in *IEEE International Conference on Robotics and Automation*, 2006, pp. 505–511.
- [7] M. J. Stealey, A. Singh, M. A. Batalin, B. Jordan, and W. J. Kaiser, "NIMS3D: A novel system for autonomous sensing of aquatic environments," in *IEEE/RSJ International Conference on Robotics and Automation*, 2008.
- [8] P. Bosscher, R. L. Williams, and M. Tummino, "A concept for rapidly-deployable cable robot search and rescue systems," in *ASME IDETC/CIE*, 2005.
- [9] "Skycam." [Online]. Available: www.skycam.tv
- [10] "Cablecam." [Online]. Available: www.cablecam.com
- [11] K. Usher, G. Winstanley, R. Carnie, P. Corke, and D. Stauffacher, "Air vehicle simulator: an application for a cable array robot," in *IEEE International Conference on Robotics and Automation*, 2005, pp. 2241–2246.
- [12] P. H. Borgstrom, M. J. Stealey, M. A. Batalin, and W. J. Kaiser, "NIMS3D: A novel rapidly deployable robot for 3-dimensional applications," in *IEEE/RSJ International Conference on Intelligent Robots and Systems*, Beijing, China, 2006, pp. 3628–3635.
- [13] P. H. Borgstrom, N. P. Borgstrom, M. J. Stealey, B. Jordan, G. Sukhatme, M. A. Batalin, and W. J. Kaiser, "Generation of energy efficient trajectories for nims3d, a three-dimensional cabled robot," in *IEEE International Conference on Robotics and Automation*, 2008.
- [14] I.-M. Chao, B. L. Golden, and E. A. Wasil, "A fast and effective heuristic for the orienteering problem," *Eur. Jour. of Op. Research*, vol. 88, pp. 475–489, 1996.
- [15] "Geo brick manual." [Online]. Available: [http://www.deltatau.com/fmenu/Geo Brick User.pdf](http://www.deltatau.com/fmenu/Geo%20Brick%20User.pdf)
- [16] S. Cetinkunt, *Mechatronics*. John Wiley & Sons, Inc., 2007.
- [17] G. Dantzig, A. Orden, and P. Wolfe, "Generalized simplex method for minimizing a linear form under linear inequality constraints," *Pacific Journal Math*, vol. 5, no. 2, pp. 183–195, 1955.
- [18] R. L. Panton, *Incompressible Flow*, 2nd ed. Wiley Interscience, 1996.
- [19] "Parker motor specification sheet." [Online]. Available: http://apps.parker.com/compumotor/cat/english/SM_SeriesMotor.pdf
- [20] "Cleveland kidder tension gauges." [Online]. Available: http://www.cmcontrols.com/downloads/web_tension_control/ds_ultra_clt.pdf
- [21] C. E. Rasmussen and C. K. Williams, *Gaussian Process for Machine Learning*, ser. Adaptive Computation and Machine Learning. MIT Press, 2006.
- [22] W. Caselton and J. Zidek, "Optimal monitoring network design," *Statistics and Probability Letters*, 1984.
- [23] A. Krause, A. Singh, and C. Guestrin, "Near-optimal sensor placements in Gaussian processes: Theory, efficient algorithms and empirical studies," in *JMLR*, 2007.
- [24] Y.-C. Liang, S. Kulturel-Konak, and A. E. Smith, "Meta heuristics for the orienteering problem," in *Proceedings of Congress on Evolutionary Computation (CEC)*, 2002, pp. 384–389.
- [25] A. Krause and C. Guestrin, "Nonmyopic active learning of gaussian processes: an exploration-exploitation approach," in *International Conference on Machine Learning (ICML)*, 2007, pp. 449–456.